

Electronic Supplementary Information

***In situ* Electrochemical Formation of Core-Shell Nickel-Iron Disulfide and Oxyhydroxide Heterostructured Catalysts for Stable Oxygen Evolution Reaction and the Associated Mechanisms**

Min Zhou, Qunhong Weng\*, Xiuyun Zhang, Xi Wang\*, Xianghua Zeng, Yoshio Bando and Dmitri Golberg\*

**Table S1. Comparison of OER catalytic performances of Ni-Fe pyrite with the literature data.**

Materials	Overpotential # (mV)	Tafel slope (mV/dec)	Stability	References
Co <sub>3</sub> O <sub>4</sub> -Carbon Porous Nanowire	290	70	<i>j</i> : 6.5% loss at 1.52 V (vs. RHE) after 30 h	<i>J. Am. Chem. Soc.</i> <b>2014</b> , <i>136</i> , 13925.
CoSe <sub>2</sub> Nanosheets	320	44	----	<i>J. Am. Chem. Soc.</i> <b>2014</b> , <i>136</i> , 15670.
Ni-Fe hydroxides /N-Doped graphene	337	45	<i>j</i> : ~7 % loss at η=350 mV after 3.3 h	<i>Adv. Mater.</i> <b>2015</b> , <i>27</i> , 4516.
Fe-Doped Ni Oxide Nanocrystals	297	37	----	<i>ACS Nano</i> <b>2015</b> , <i>9</i> , 5180.
Ni-Fe oxide	328	42	<i>j</i> : no obvious change at 1.62 V (vs. RHE) after 12 h	<i>Adv. Sci.</i> <b>2015</b> , <i>2</i> , 1500199
Ni-Fe LDH/rGO	210	42	V: 20 mV increment at <i>j</i> =10 mA/cm <sup>2</sup> after 10h	<i>ACS Nano</i> <b>2015</b> , <i>9</i> , 1977.
Ni-Fe alloy/graphene	280	70	----	<i>Energy Environ. Sci.</i> <b>2016</b> , <i>9</i> , 123.
CoSn(OH) <sub>6</sub> nanocubes	274	----	<i>j</i> : no obvious change at η=313 mV after 11 h	<i>Energy Environ. Sci.</i> <b>2016</b> , <i>9</i> , 473.
Ni <sub>3</sub> FeN nanoparticle	280	46	<i>j</i> : ~6 % loss at η=284 mV after 9 h	<i>Adv. Energy Mater.</i> <b>2016</b> , DOI: 10.1002/aenm.201502585.
Fe <sub>3</sub> O <sub>4</sub> @Co <sub>9</sub> S <sub>8</sub> /rGO	340	54.5	<i>j</i> : 12 % loss at η=320 mV after 6 h	<i>Adv. Funct. Mater.</i> <b>2016</b> , DOI: 10.1002/adfm.201600674.
(Co <sub>1-x</sub> Fe <sub>x</sub> ) <sub>2</sub> P	270	30	----	<i>Energy Environ. Sci.</i> <b>2016</b> , DOI: 10.1039/C6EE01109H.
Gelled-FeCoW	223	37	V: no obvious change at <i>j</i> =30 mA/cm <sup>2</sup> after 550 h	<i>Science</i> <b>2016</b> , DOI: 10.1126/science.aaf1525.
Ni-Fe disulfide @oxyhydroxide	<b>230</b>	<b>42.6</b>	<b>V: 10 mV increment at <i>j</i>=10 mA/cm<sup>2</sup> after 50 h</b>	<b>This work</b>

# obtained on glassy carbon electrode, at a current density of 10 mA/cm<sup>2</sup>.

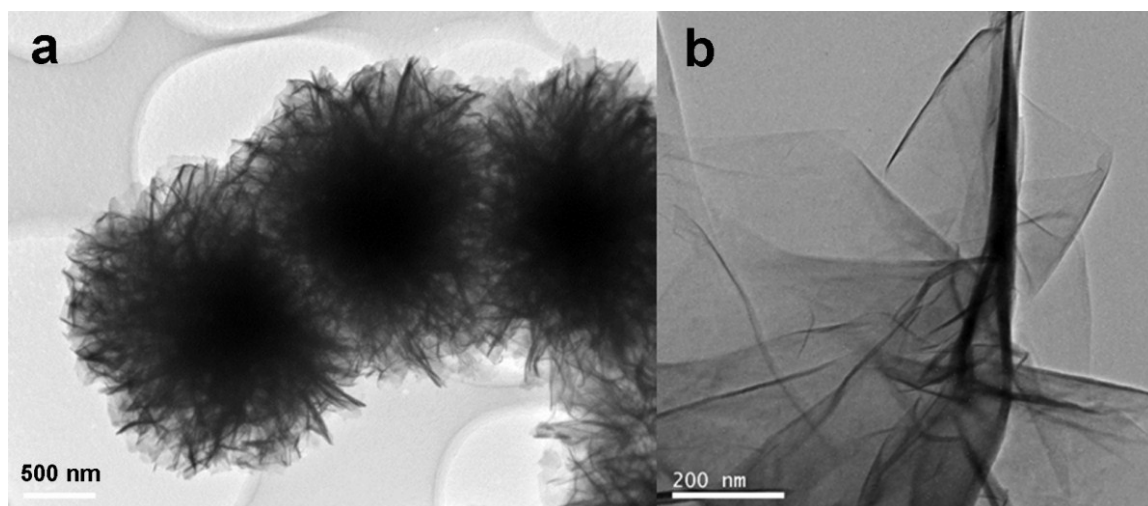


Figure S1. TEM images of a Ni-Fe hydroxide precursor.

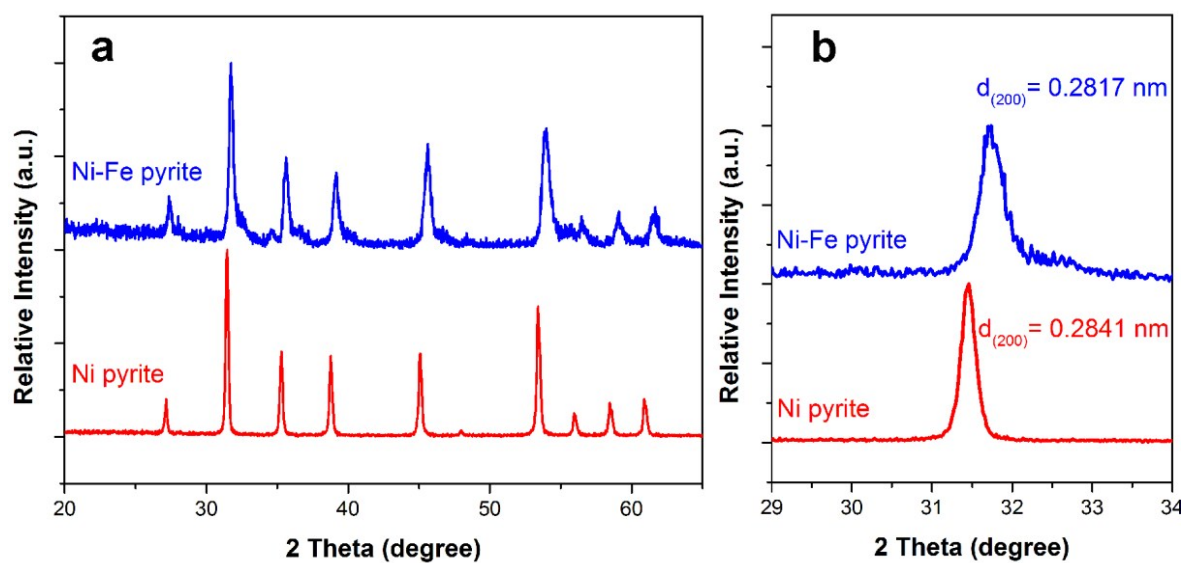
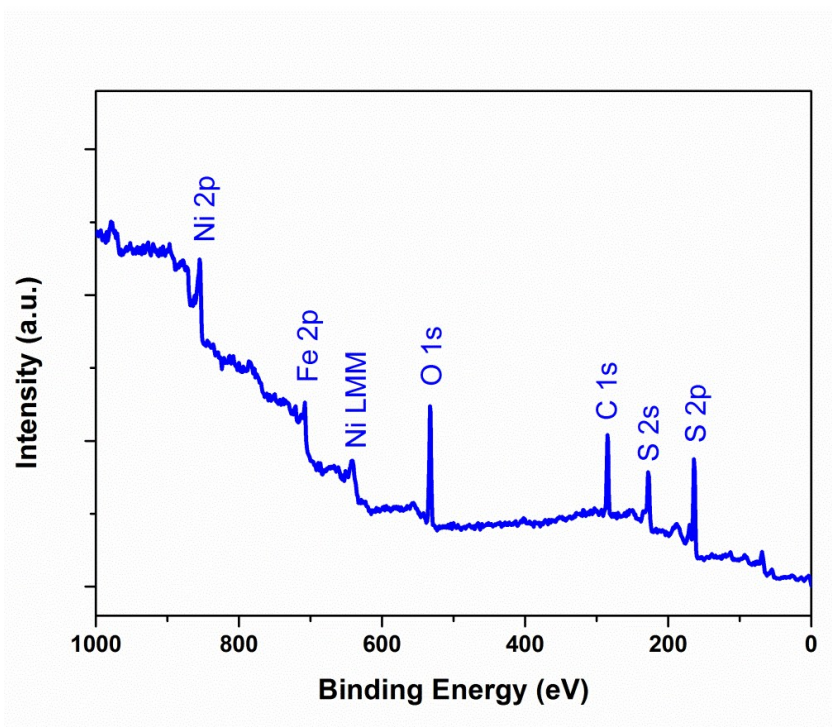
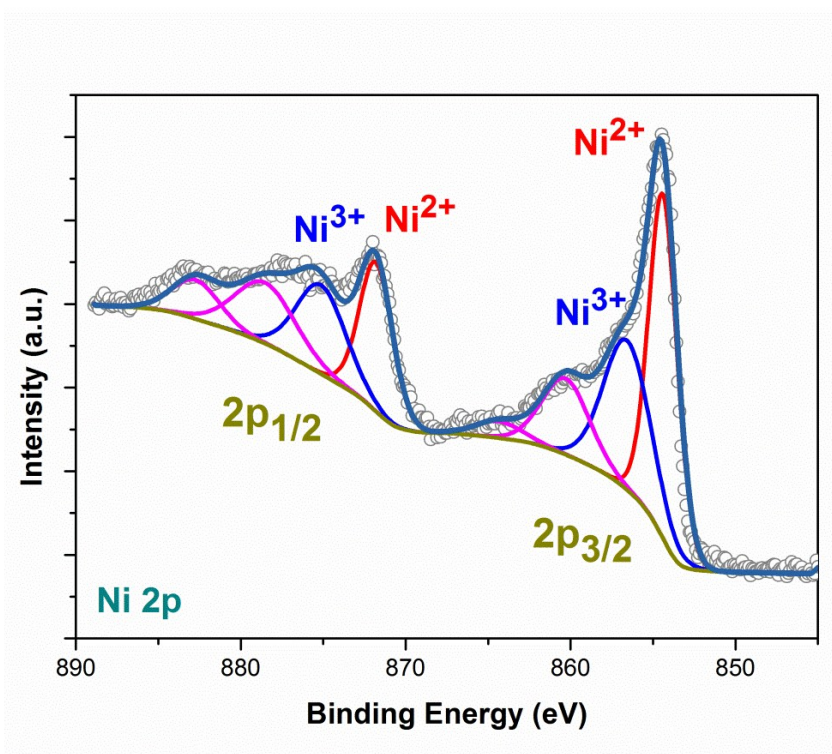


Figure S2. (a) XRD patterns of Ni-Fe pyrite and Ni pyrite. (b) (200) peak shift of the Ni-Fe pyrite.



**Figure S3.** Wide-range XPS spectrum of a Ni-Fe disulfide.



**Figure S4.** XPS spectrum of Ni 2p of Ni disulfide. Slight peak shifts are observed with respect to the Ni-Fe disulfide peaks. The binding energies of Ni<sup>2+</sup> 2p<sub>3/2</sub> and 2p<sub>1/2</sub> in Ni disulfide are 854.5 and 871.9 eV, respectively. These values shift to 854.2 and 871.6 eV in the Ni-Fe bi-metal disulfide.

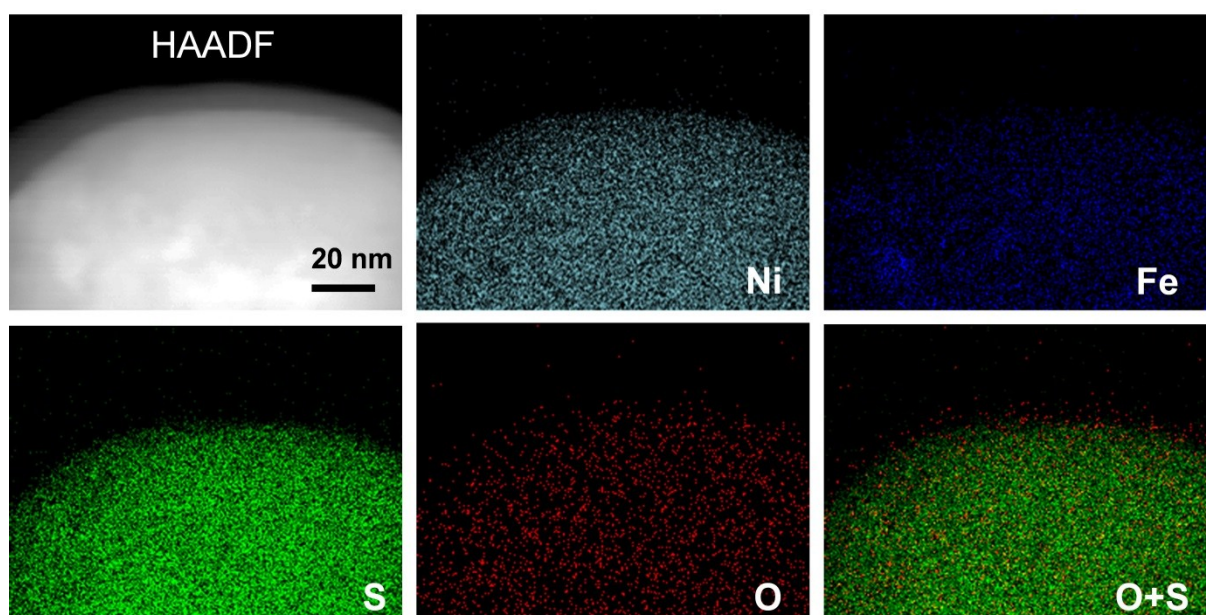


**Figure S5.** Elemental mapping of the Ni-Fe disulfide after the 1<sup>st</sup> OER cycle.

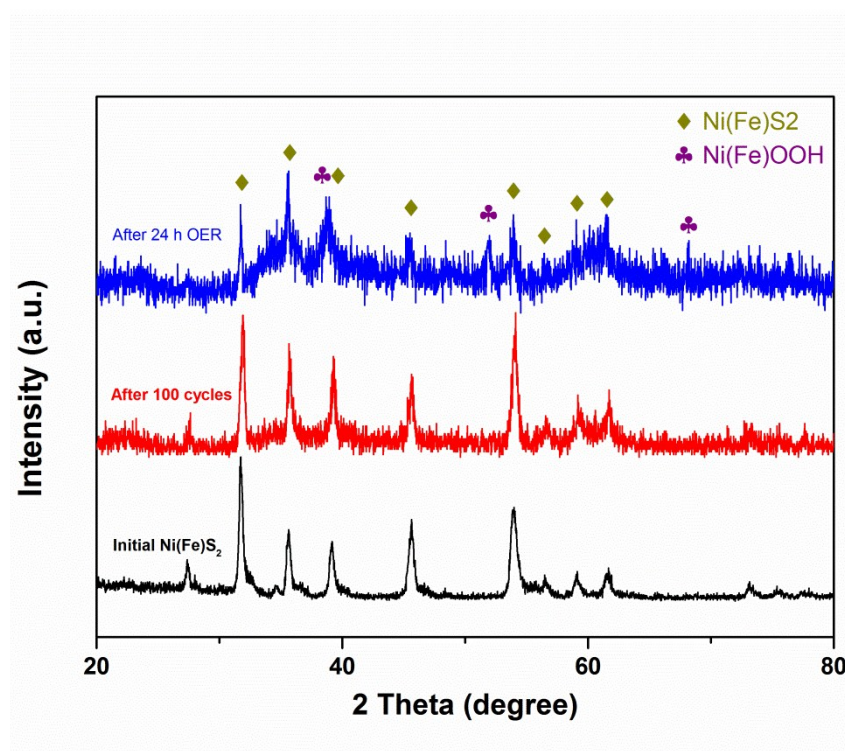


**Figure S6.** XRD patterns of the initial Ni(Fe)S<sub>2</sub>, the catalysts after 100 OER cycles and 24 h OER stability test. After 24 h OER stability test, the main phase of the catalyst is still Ni(Fe)S<sub>2</sub>. However, the weak diffraction peaks of crystalline Ni(Fe)OOH (JCPDS: 06-0075) were also observed in the pattern of the catalyst after 24 h OER, indicating the formation of a Ni(Fe)OOH phase in addition to the existence of original Ni(Fe)S<sub>2</sub>. In the sample after 100 OER cycles, the diffraction patterns

belonging to the Ni(Fe)OOH phase were not observed. This is because the initially formed shell Ni(Fe)OOH structure is mainly amorphous.

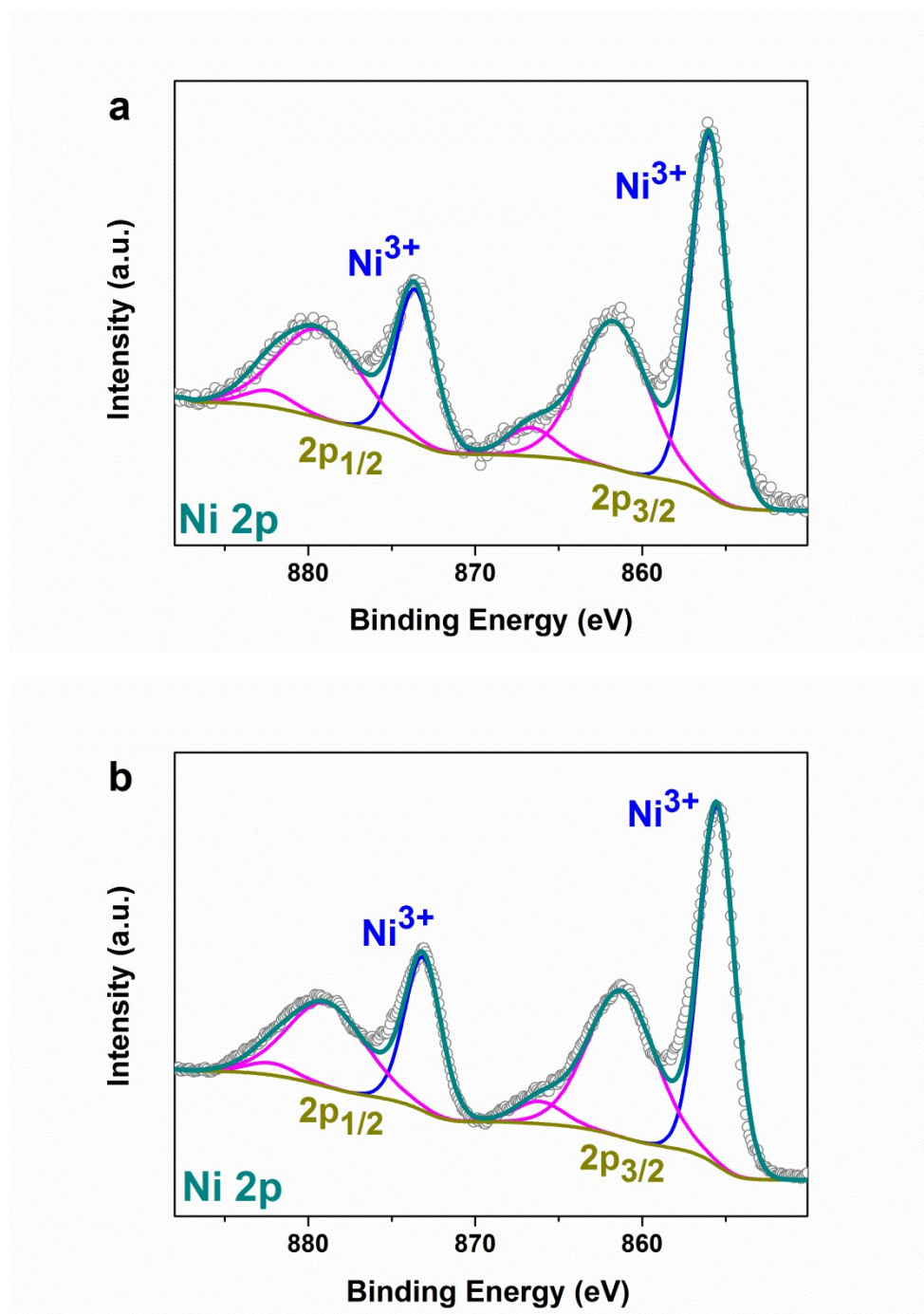


**Figure S7.** XPS spectra of Ni 2p from the catalysts after 100 OER cycles (a) and 24 h OER stability test (b). The binding energies reveal the presence of Ni<sup>3+</sup> cations (855.5 and 873.3 eV) in the catalysts, consistent with the valence states of NiOOH. Other fitted peaks (magenta lines) are satellite peaks of Ni 2p<sub>1/2</sub> and 2p<sub>3/2</sub>. Different from the valence states of the initial Ni(Fe)S<sub>2</sub> catalyst (Figure 1c), we have not observed any peaks attributed to Ni<sup>2+</sup>. This is because XPS reflects the surface information from a material. And the new catalytic surface containing Ni<sup>3+</sup> was formed.

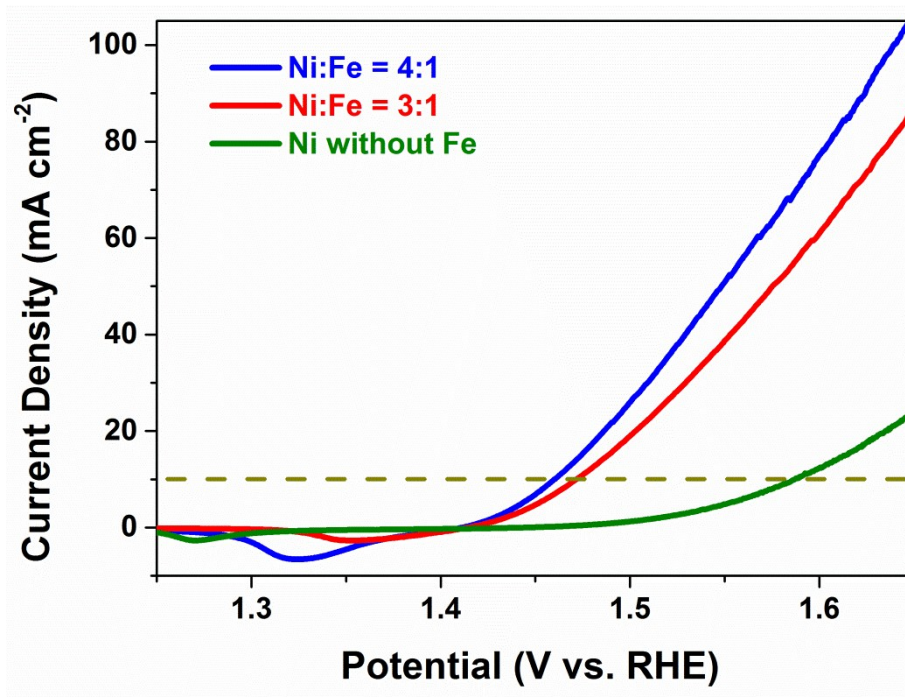


**Figure S8.** Normalized LSV polarization curves of Ni-Fe disulfide@oxyhydroxides with varied Fe contents.

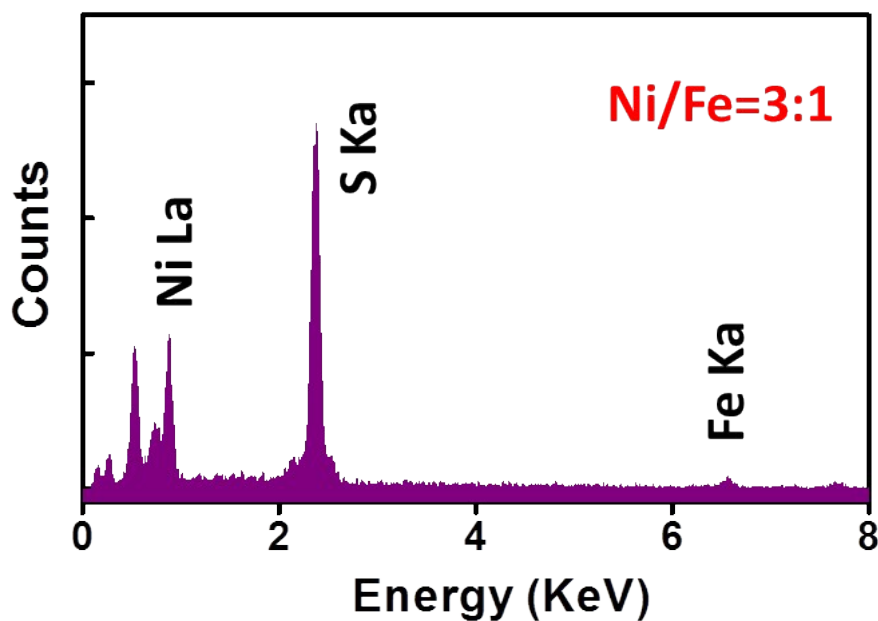


**Figure S9.** EDX spectrum of a Ni-Fe disulfide with the increased Fe content, this reveals a Ni:Fe molar ratio of 3:1.

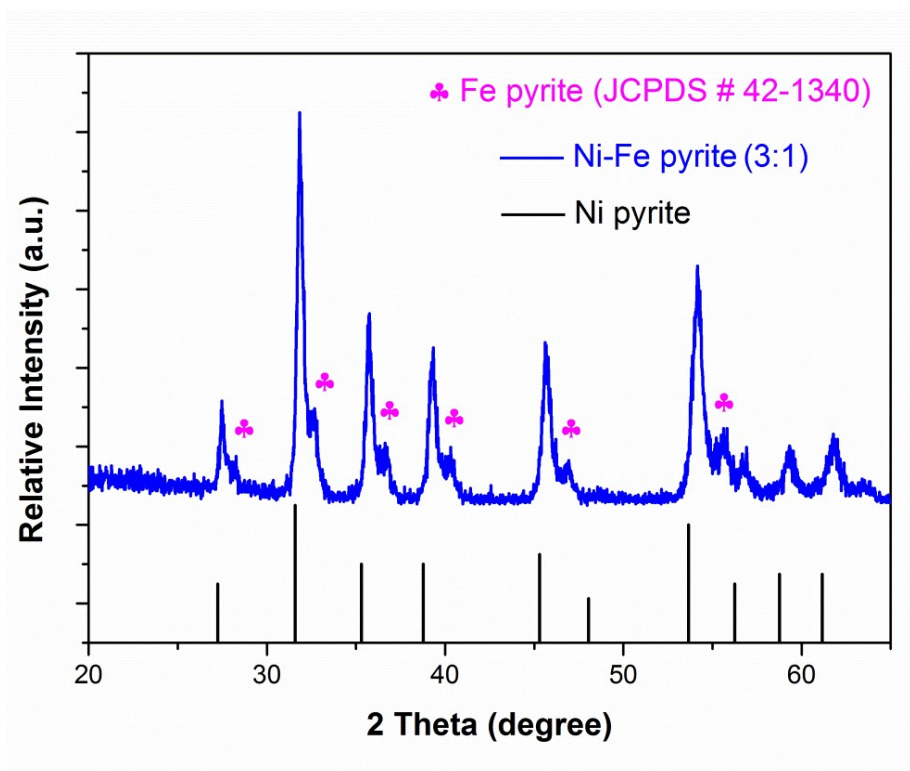


**Figure S10.** XRD pattern of a Ni-Fe pyrite with a Ni:Fe molar ratio of 3:1. The magenta marks indicate the presence of Fe pyrite phase ( $\text{FeS}_2$ ).

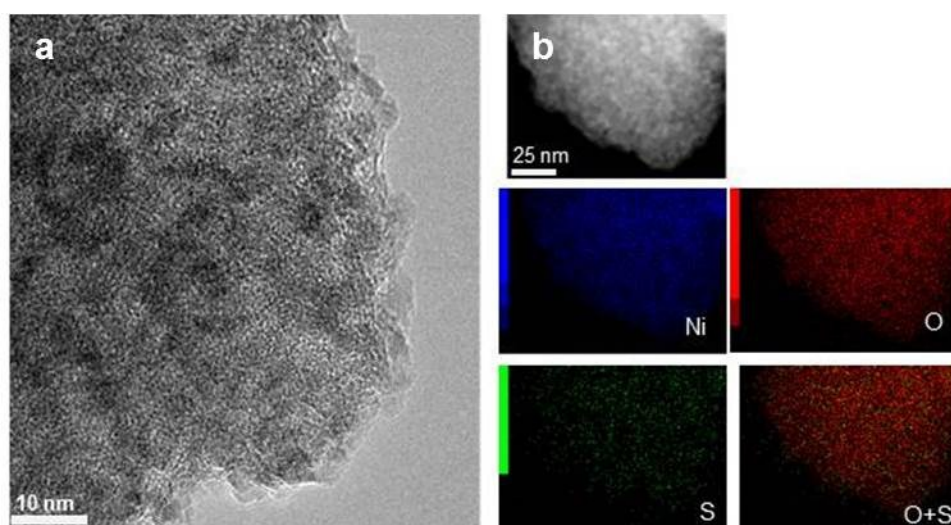


**Figure S11.** (a) HRTEM image of a Ni disulfide after amperometric OER stability experiment for 24 h. (b) Elemental maps of Ni disulfide after amperometric OER experiment for 24 h. Oxygen is dispersed over the whole particle, as revealed by elemental mapping, this indicates that nickel sulfide was almost completely converted after 24 OER. This data demonstrates that introducing iron not only boosts the catalytic activity, but also hinders the phase transformation during OER.

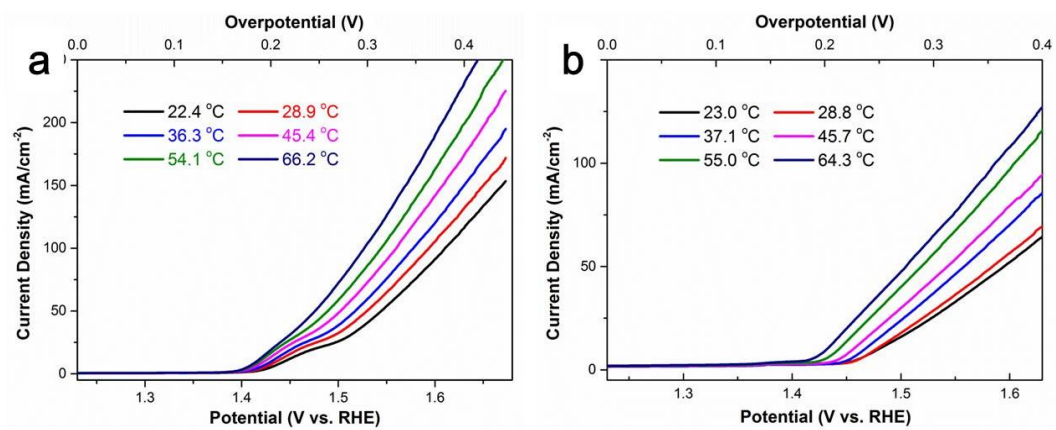


**Figure S12.** Temperature-dependent catalytic activity of (a) a Ni-Fe disulfide@oxyhydroxide and (b) a hydroxide.